

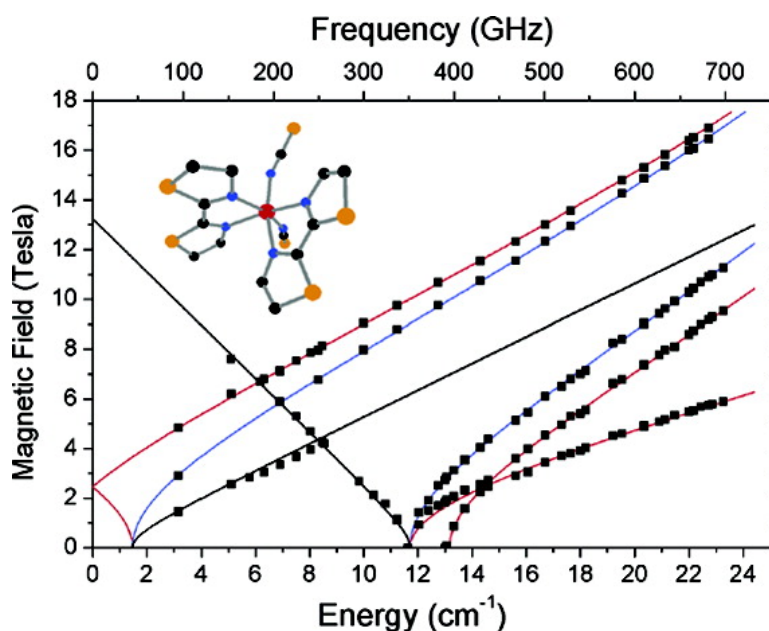
Communication

High-Frequency and -Field EPR of a Pseudo-octahedral Complex of High-Spin Fe(II): Bis(2,2'-bi-2-thiazoline)bis(isothiocyanato)iron(II)

Andrew Ozarowski, S. A. Zvyagin, William M. Reiff, Joshua Telser, Louis-Claude Brunel, and J. Krzystek

J. Am. Chem. Soc., **2004**, 126 (21), 6574-6575 • DOI: 10.1021/ja048336m • Publication Date (Web): 08 May 2004

Downloaded from <http://pubs.acs.org> on March 31, 2009



More About This Article

Additional resources and features associated with this article are available within the HTML version:

- Supporting Information
- Links to the 2 articles that cite this article, as of the time of this article download
- Access to high resolution figures
- Links to articles and content related to this article
- Copyright permission to reproduce figures and/or text from this article

[View the Full Text HTML](#)

High-Frequency and -Field EPR of a Pseudo-octahedral Complex of High-Spin Fe(II): Bis(2,2'-bi-2-thiazoline)bis(isothiocyanato)iron(II)

Andrew Ozarowski,[§] S. A. Zvyagin,[§] William M. Reiff,[†] Joshua Telser,[‡] Louis-Claude Brunel,[§] and J. Krzystek^{*§}

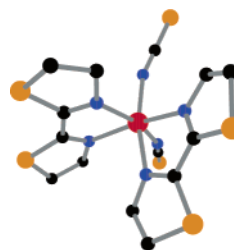
National High Magnetic Field Laboratory, Florida State University, Tallahassee, Florida 32310, Department of Chemistry and Chemical Biology, Northeastern University, Boston, Massachusetts 02115, and Chemistry Program, Roosevelt University, Chicago, Illinois 60605

Received March 23, 2004; E-mail: krzystek@magnet.fsu.edu

Iron is ubiquitous in metalloproteins, in a wide range of coordination environments. A large and important class of Fe proteins consists of the non-heme Fe proteins, in which Fe is often six-coordinate and generally has two or more endogenous histidine ligands.^{1,2} HS³ Fe(II) (3d⁶, *S* = 2) is an important state in non-heme Fe proteins; however, this state is relatively difficult to investigate by EPR, normally a technique of choice for paramagnetic transition metal systems. HS Fe(II) is a non-Kramers (integer spin) ion of typically large zfs, on the order of 5–20 cm⁻¹.^{4,5} The allowed EPR transitions thus generally appear at high frequencies, and/or at high magnetic fields.⁶ Among spectroscopic methods generally applied to HS Fe(II) systems, Mössbauer spectroscopy^{7,8} and MCD^{1,9} are most informative, as are magnetic susceptibility measurements.¹⁰ Far-infrared (FIR) spectroscopy¹¹ and, more recently, INS¹² have also been employed to detect transitions among the HS Fe(II) quintet-state zero-field levels and consequently provide information on its electronic structure. Another approach is to employ EPR, but at frequencies and fields sufficiently high to observe the allowed transitions.¹³ Successful HFEPR of HS Fe(II) is still infrequent, with one study on a pseudo-tetrahedral complex, [PPh₄]₂[Fe(SPh₄)], a model for reduced rubredoxin,¹⁴ and one on an octahedral complex, [Fe(im)₆](NO₃)₂.¹² The HFEPR results in the latter report were, however, secondary to highly informative INS results. Very few HFEPR transitions were observed, and the S/N ratio of reported EPR spectra was relatively low.¹² We demonstrate here that it is indeed possible to observe multiple HFEPR transitions for HS Fe(II) with high S/N ratio, in this case for a *cis*-FeN₂N₄ chromophore complex: bis(2,2'-bi-2-thiazoline)-bis(isothiocyanato)iron(II) (**1**). Complex **1** can be considered as an approximate model for six-coordinate active sites in non-heme Fe proteins, wherein their histidine ligands are represented in **1** by the imino N-donor thiazoline ligands. We show that it is possible by HFEPR to accurately determine spin Hamiltonian parameters in this complex, and relate them to the electronic structure.

Complex **1** exists as two polymorphs, A^{15–18} and B.¹⁸ It was polymorph A that drew initial attention since it undergoes a temperature-driven spin-crossover transition to a diamagnetic (LS, *S* = 0) state.^{15–18} Polymorph B remains paramagnetic (HS, *S* = 2) to 4.2 K but is “silent” at conventional EPR frequencies. Crystals of each polymorph can be independently prepared, and their structures have been determined.¹⁸ The structure of polymorph B (**1B**) is shown in Chart 1. Crystals of **1B** were ground to a fine powder for HFEPR experiments. The HFEPR apparatus and the tunable-frequency EPR methodology as employed here have been previously described.¹⁹ We have also performed Mössbauer spec-

Chart 1. Molecular Structure of **1B**



troscopy measurements at 77 and 293 K, and DC SQUID magnetometry between 1.8 and 293 K for **1B**.

Figure 1 shows typical HFEPR spectra of **1B** using two different modulation techniques: chopping the sub-THz wave beam, which results in an absorptive shape (black trace), and standard modulation of magnetic field (blue trace). The red trace is a derivative simulation (see below) assuming a perfect powder pattern. The agreement between magnetically modulated spectra and their simulation is very good in terms of resonance position, but less so in terms of line shape. We find that modulation results in fast-passage effects²⁰ at low temperatures, which strongly distort the line shapes. The HFEPR spectra at sufficiently high operating frequencies consist of five strong, well-defined resonances. In addition, some weaker and narrower lines appear in the *g* = 2 region of the spectra (22 T at 610 GHz, not shown), which belong to a Kramers-type impurity, most probably HS Fe(III).²¹ Rather than fitting the spin Hamiltonian parameters to single-frequency spectra, we obtained a two-dimensional dataset of the resonant fields versus transition energies, as shown by the squares in Figure 2. A peculiarity of this dataset is the two zero-field transitions observed at ca. 11.5 and 13.0 cm⁻¹, respectively. By analogy with the zero-field FIR results on ferrous fluorosilicate,¹¹ we attribute these transitions to those between the |0'⟩ and the |1^a⟩ and |1^b⟩ levels, respectively,²² yielding initial zfs parameters: |*D*| = 12.25, |*E*| = 0.25 cm⁻¹ (the zero-field energy level diagram for *S* = 2 is illustrated by Figure S1 in Supporting Information). Subsequent refinement by simultaneously fitting the standard spin Hamiltonian⁴ parameters to the complete dataset of HFEPR resonances yields: *D* = +12.427(12), *E* = +0.243(3) cm⁻¹; *g*_x = 2.147(3), *g*_y = 2.166(3), *g*_z = 2.01(1), which produces the simulated curves in Figure 2. The *g* values are greater than 2.00, as expected for a more than half-filled d-shell electron configuration. The remarkable agreement between the simulations and experiment allows us to attribute each of the resonance branches observed experimentally to particular turning points in a quintet state manifold powder pattern.

The quadrupole splitting of the ⁵⁷Fe Mössbauer spectrum of **1B** (Figure S2) is relatively temperature independent and has a value

[§] Florida State University.

[†] Northeastern University.

[‡] Roosevelt University.

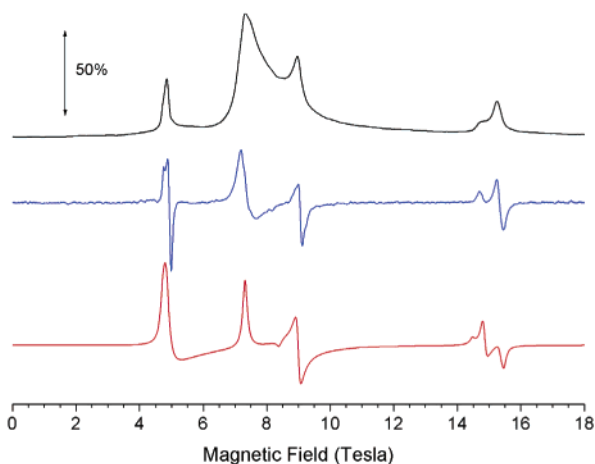


Figure 1. HFEPR spectra of polymorph B of **1** at 610 GHz and 10 K using optical modulation (black trace), and magnetic modulation (blue trace). The red trace shows a simulation of the magnetically modulated spectrum using spin Hamiltonian parameters: $D = +12.427$, $E = +0.243$ cm^{-1} ; $g_x = 2.147$, $g_y = 2.166$, $g_z = 2.01$, and assuming a powder pattern distribution. A bar representing a 50% absorption value is included next to the optically modulated spectrum.

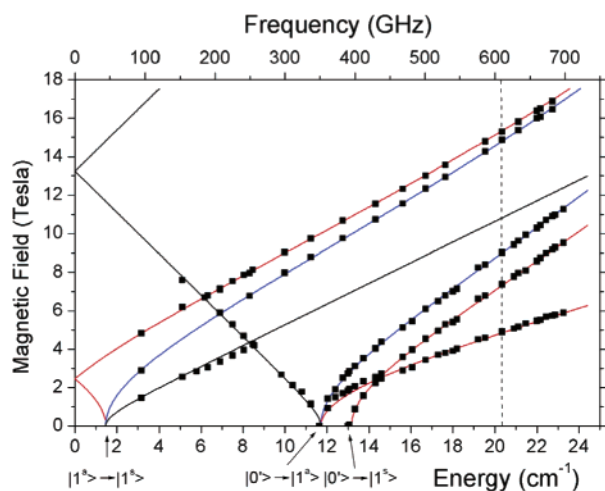


Figure 2. Resonance field vs sub-THz wave quantum energy dependence for EPR transitions in polymorph B of **1**. Experimental points are represented by squares. Simulations using spin Hamiltonian parameters as in Figure 1 are shown by blue lines for x turning points, red lines for y turning points, and black lines for z turning points. Three zero-field resonances, of which two are observable in the 95–700 GHz range, are labeled accordingly. The dashed line at 610 GHz, parallel to the Y axis, reproduces the resonances shown in Figure 1.

of ~ 3.00 mm/s at 77.5 K, similar to the limiting value found¹⁶ for the HS form of polymorph A. This is consistent with an isolated, orbitally nondegenerate ground state and the expectation of essentially spin-only magnetic behavior at low temperature. DC susceptibility shows temperature dependence of μ_{eff} that can be fit to $D \approx +12$ cm^{-1} (Figure S3).

Our results show for the first time that HFEPR can detect strong, well-defined resonances of HS Fe(II) in a pseudo-octahedral complex characterized by a large, positive D , as corroborated by Mössbauer and magnetic susceptibility studies. The tunable-frequency HFEPR methodology allows for the detection of zero-field resonances, affords easy identification of transitions, and yields highly accurate spin Hamiltonian parameters. These parameters can give initial insight into the electronic structure of Fe(II) in **1B**.

Taking as a starting point the detailed ligand-field analysis of $[\text{Fe}(\text{im})_6](\text{NO}_3)_2$ by Carver et al.,¹² we use the full d^6 basis set and the following parameters moderately altered from theirs,¹² chiefly by including a larger trigonal splitting (values in cm^{-1}): Racah $B = 750$, $C = 3400$; Ballhausen crystal-field, $Dq = 1100$,¹⁷ $Ds = 370$, and spin-orbit coupling, $\zeta = 368$ ($\lambda = -92$), which yield a true spin quintet, orbitally nondegenerate ground state with axial zfs, $D = +12.5$ cm^{-1} . The heteroleptic nature of **1** as opposed to homoleptic $[\text{Fe}(\text{im})_6]^{2+}$ makes an AOM analysis¹² more difficult in our case, and we have not attempted it, nor have we tried to model the small rhombic zfs term observed. Nevertheless, the results described here, together with those of Carver et al.,¹² suggest a commonality in electronic structure of HS Fe(II) complexes with N_6 coordination and, more generally, that HFEPR, at least in certain propitious cases such as complex **1B**, can and should be added to the armamentarium of techniques for investigating HS Fe(II) complexes side-by-side with well-established methods.^{1,7–9}

Acknowledgment. NHMFL is funded by the NSF through Grant DMR9016241. NSF-DMR supported the purchase of a SQUID magnetometer at Northeastern University. The W. M. Keck Foundation funded the high-homogeneity resistive magnet.

Supporting Information Available: Energy level diagram for $S = 2$ and Mössbauer and magnetic susceptibility results on **1B**. This material is available free of charge via the Internet at <http://pubs.acs.org>.

References

- (1) Solomon, E. I. *Inorg. Chem.* **2001**, *40*, 3656–3669.
- (2) Ryle, M. J.; Hausinger, R. P. *Curr. Opin. Struct. Biol.* **2002**, *9*, 722–731.
- (3) Abbreviations used: AOM, angular overlap model; EPR, electron paramagnetic resonance; FIR, far-infrared; HFEPR, high-frequency and -field EPR.; HS, high-spin; im, imidazole; INS, inelastic neutron scattering; LS, low-spin; MCD, magnetic circular dichroism; S/N, signal-to-noise; zfs, zero-field splitting.
- (4) Abragam, A.; Bleaney, B. *Electron Paramagnetic Resonance of Transition Ions*; Dover Publications: New York, 1986.
- (5) Hendrich, M.; Debrunner, P. *Biophys. J.* **1989**, *56*, 489–506.
- (6) An exception is the “non-Kramers transition” between the $[M_S] = 2$ levels, which is observed at conventional frequencies, e.g. at X-band (9 GHz), at very low magnetic fields, for specific conditions of zfs tensor rhombicity.
- (7) Long, G. J., Ed. *Mössbauer Spectroscopy Applied to Inorganic Chemistry*; Plenum Press: New York, 1984; Vol. 1.
- (8) Münck, E.; Surerus, K. K.; Hendrich, M. P. *Methods Enzymol., Part D* **1993**, *227*, 463–479.
- (9) Solomon, E. I.; Brunold, T. C.; Davis, M. I.; Kemsley, J. N.; Lee, S.-K.; Lehnert, N.; Neese, F.; Skulan, A. J.; Yang, Y.-S.; Zhou, J. *Chem. Rev.* **2000**, *100*, 235–350.
- (10) Carlin, R. L. *Magnetochemistry*; Springer: Berlin, Heidelberg, 1986.
- (11) Champion, P. M.; Sievers, A. J. *J. Chem. Phys.* **1977**, *66*, 1819–1825.
- (12) Carver, G.; Tregenna-Piggott, P. L. W.; Barra, A.-L.; Neels, A.; Stride, J. A. *Inorg. Chem.* **2003**, *42*, 5771–5777.
- (13) Riedi, P. C.; Smith, G. M. In *Electron Paramagnetic Resonance*; Gilbert, B. C.; Davies, M. J.; Murphy, D. M., Eds.; Royal Society of Chemistry: Cambridge, UK, 2002; Vol. 18, pp 254–303.
- (14) Knapp, M. J.; Krzystek, J.; Brunel, L.-C.; Hendrickson, D. N. *Inorg. Chem.* **2000**, *39*, 281–288.
- (15) Müller, E. W.; Spiering, H.; Gütlich, P. *J. Chem. Phys.* **1983**, *79*, 1439–1443.
- (16) König, E.; Ritter, G.; Irlner, W.; Nelson, S. M. *Inorg. Chim. Acta* **1979**, *37*, 169–179.
- (17) Bradley, G.; McKee, V.; Nelson, S. M.; Nelson, J. J. *Chem. Soc., Dalton Trans.* **1978**, 522–526.
- (18) Ozarowski, A.; McGarvey, B. R.; Sarkar, A. B.; Drake, J. E. *Inorg. Chem.* **1988**, *27*, 628–635; Ozarowski, A.; McGarvey, B. R.; Sarkar, A. B.; Drake, J. E. *Inorg. Chem.* **1988**, *27*, 2560–2560; Marsh, R. E. *Inorg. Chem.* **1988**, *27*, 2902–2903.
- (19) Krzystek, J.; Zvyagin, S. A.; Ozarowski, A.; Fiedler, A. T.; Brunold, T. C.; Telsler, J. *J. Am. Chem. Soc.* **2004**, *126*, 2148–2155.
- (20) Mailer, C.; Hoffman, B. M. *J. Phys. Chem.* **1976**, *80*, 842–846.
- (21) The combined susceptibility and Mössbauer spectroscopy data confirm that Fe(III) is present only at a low level (<1%).
- (22) This labeling follows the convention of Hendrich and Debrunner⁵ (see Figure S1). The $|1^{\Delta_g}\rangle \rightarrow |1^{\Delta_g}\rangle$ resonance at 1.5 cm^{-1} is outside our frequency range, and so are additional resonances appearing at much higher frequencies.

JA048336M